**Journal: Brain Stimulation (IF 6.9)**

# Transcranial direct current stimulation facilitates response inhibition through dynamic modulation of the fronto-basal ganglia network

Abbreviated title: Brain stimulation and response inhibition

Marco Sandrini*[1,2,3], Benjamin Xu*§[1,2], Rita Volochayev[1], Oluwole Awosika[1], Wen-Tung Wang[2], John A. Butman[2,4], and Leonardo G. Cohen[1]

[1]Human Cortical Physiology and Neurorehabilitation Section, National Institute of Neurological Disorders and Stroke, National Institutes of Health, Bethesda, Maryland 20892, US

[2]Center for Neuroscience and Regenerative Medicine, Uniformed Services University of Health Sciences, Bethesda, Maryland 20814, US

[3]Department of Psychology, University of Roehampton, London SW15 4JD, UK

[4]Radiology and Imaging Sciences, National Institutes of Health, Clinical Center, Bethesda, Maryland 20892, US

* These authors share first authorship

§ Corresponding author: Benjamin Xu, Ph.D.; National Institutes of Health, 6700B Rockledge, Bethesda, MD 20892; Tel: 301-443-6545; Email: benxu1@mail.nih.gov

Conflict of interest: The authors declare no competing financial interests

## Abstract

Background: Response inhibition refers to the ability to stop an on-going action quickly when it is no longer appropriate. Previous studies showed that transcranial direct current stimulation (tDCS) applied with the anode over the right inferior frontal cortex (rIFC), a critical node of the fronto-basal ganglia inhibitory network, improved response inhibition. However, the tDCS effects on brain activity and network connectivity underlying this behavioral improvement are not known.

Objective: This study aimed to address the effects of tDCS applied with the anode over the rIFC on brain activity and network functional connectivity underlying the behavioral change in response inhibition.

Methods: Thirty participants performed a stop-signal task in a typical laboratory setting as a baseline during the first study visit (i.e., Session 1). In the second visit (at least 24 hours after Session 1), all participants underwent resting-state functional magnetic resonance imaging (rsfMRI) scans before and after 1.5 mA tDCS (Anodal or Sham). Immediately following the post-tDCS rsfMRI, participants performed the same stop-signal task as in Session 1 during an event-related fMRI (efMRI) scan in a 3T scanner. Changes in task performance, i.e., the stop-signal response time (SSRT), a measure of response inhibition efficiency, was determined relative to the participants' own baseline performance in Session 1.

Results: Consistent with previous findings, Anodal tDCS facilitated the SSRT. efMRI results showed that Anodal tDCS strengthened the functional connectivity between right pre-supplementary motor area (rPreSMA) and subthalamic nuclei during Stop responses. rsfMRI revealed changes in intrinsic connectivity between rIFC and caudate, and between rIFC,

rPreSMA, right inferior parietal cortex (rIPC), and right dorsolateral prefrontal cortex (rDLPFC) after Anodal tDCS. In addition, corresponding to the regions of rsfMRI connectivity change, the efMRI BOLD signal in the rDLPFC and rIPC during Go responses accounted for 74% of the variance in SSRT after anodal tDCS, indicating an effect of tDCS on the Go-Stop process.

Conclusion: These results indicate that tDCS with the anode over the rIFC facilitates response inhibition by modulating neural activity and functional connectivity in the fronto-basal ganglia as well as rDLPFC and rIPC as an integral part of the response inhibition network.

Key words: tDCS; fMRI; brain stimulation; prefrontal cortex; response inhibition; inhibitory control

## Introduction

Response inhibition refers to the ability to stop an on-going action quickly when it is no longer appropriate (1) and is one of the core components of the human executive function that regulates the dynamics of actions (2). This ability may be significantly impaired after brain injuries or disorders affecting the fronto-basal ganglia inhibitory circuits, such as traumatic brain injury, drug addiction, attention deficit/hyperactivity disorder, and obsessive-compulsive disorder (3-9).

A common research paradigm to measure the ability to stop a response rapidly is the stop-signal task (1, 10). During this task, subjects are instructed to respond as quickly as possible to the primary Go stimuli. Occasionally, a stop signal is presented (e.g. a visual cue) shortly after the onset of a primary Go stimulus. Subjects are instructed to try to stop their response as soon as the stop signal appears. The efficiency of response inhibition is estimated using the stop-signal response time (SSRT) (10, 11). Shorter SSRT indicates more efficient response inhibition.

Accumulating evidence has shown that stopping an on-going response engages a fronto-basal ganglia network which includes the right inferior frontal cortex (rIFC), the pre-supplementary motor area (preSMA), and the basal ganglia, especially the subthalamic nucleus (STN) (7, 12, 13). The importance of rIFC has been supported by lesion (Aron et al., 2003) and transcranial magnetic stimulation (TMS) studies (14-16). Specifically, disruption of the rIFC decreased the efficiency of response inhibition (i.e. longer SSRT). Other studies further showed that transcranial direct current stimulation (tDCS) using a cephalic montage with the anode over the rIFC and cathode over the left supraorbital region improved response inhibition (i.e.

shorter SSRT) (17-20). However, the tDCS effects on brain activity and network connectivity underlying this behavioral improvement are not known.

Like other non-invasive brain stimulation techniques such as TMS (21, 22), tDCS influences interactions between interconnected brain regions beyond the targeted area (23-25). For example, it has been shown that tDCS applied with the anode over the preSMA, another critical node of the fronto-basal ganglia network (16, 26), increased functional coupling between the preSMA and ventromedial prefrontal cortex and facilitated response inhibition (25). Uncovering the effects of tDCS on brain activity and functional connectivity (27) associated with response inhibition is important not only for understanding the tDCS effects on this brain function but also for the development of non-invasive strategies for patients with impaired ability in inhibitory control.

In this study, subjects performed an identical stop-signal task in two experimental sessions separated by at least 24 hours. The task performance in the first session (i.e., Session 1) served as the baseline measure of the efficiency of response inhibition (i.e. SSRT) without tDCS. In the second session (i.e., Session 2), resting-state functional magnetic resonance imaging (rsfMRI) was acquired before and after tDCS (Anodal or Sham) using an electrode montage (i.e., the anode over the rIFC and cathode over the left supraorbital region) previously shown to improve response inhibition (17-20). Immediately after the second rsfMRI, subjects performed the same stop-signal task again during an event-related fMRI (efMRI) (see Figure 1). The baseline SSRT of each participant from Session 1 was subtracted from that in Session 2 (see the Statistical Analysis section below for reasons using Session 1 as baseline). The difference (Δ) in the SSRT between Session 2 and Session 1 ( SSRT) was the primary outcome measure of tDCS effect on response inhibition.

---

Insert Figure 1 about here

---

## Methods and Materials

### *Participants*

Forty-one healthy human volunteers were enrolled in this study. Eleven subjects were excluded from the final analysis (three subjects showed cysts in the structural MRI and eight did not complete both sessions or had technical problems). All remaining 30 subjects (7 males and 8 females in each group; mean age of the Anodal tDCS group = 26, SD= ±4; mean age of the Sham group = 27, SD= ±6) had a normal structural MRI, neurological examination, and were right-handed based on the evaluation with the Edinburgh Handedness Inventory (28). All subjects gave their written informed consent to participate in the study, which was approved by the Combined Neuroscience Institutional Review Board at the National Institutes of Health (NIH) and in accordance with the Declaration of Helsinki. Subjects received monetary compensation for their time participating in the study.

### *Transcranial direct current stimulation (tDCS)*

tDCS is a portable device which uses a constant low-intensity current (between 1 and 2 mA) delivered directly to the cortex via surface electrode pads with an anode and a cathode (29). tDCS applied with the anode over the primary motor cortex increases cortical excitability (30) and may facilitate behavioral performance (31). In this study, a battery-powered tDCS stimulator (1x1, Soterix Medical Inc., New York, US) delivered constant current at 1.5 mA for 20 minutes (with a ramping period of 20 seconds at the beginning and at the end of the stimulation) through a pair of saline-soaked sponge electrodes ($5 \times 5$ $cm^2$). The current

density (0.06 mA/cm$^2$) was maintained below safety limits (32). The anodal electrode pad was placed over the rIFC centering over the pars opercularis (i.e. cortex posterior to the ascending ramus of the lateral fissure), which is the region most commonly implicated in response inhibition (33). The anatomical locus of the pars opercularis was localized using each subject's T1 structural MR images at the beginning of Session 2 with a frameless sterotactic neuronavigation system (Brainsight, Rogue Reseach Inc., Montreal, Canada). This target location was then marked on the scalp using a red ink pencil. The cathodal electrode pad was placed above the left supraorbital area as done in previous studies that demonstrated enhanced response inhibition with the same cephalic montage (17-19). The electrodes were secured using elastic bands.

All subjects were naïve to the tDCS procedures. They were told prior to the study that each individual might have different sensitivity to the tDCS stimulation. For the Sham stimulation, the tDCS montage was the same as the Anodal condition, but the current was turned off 20 seconds after the beginning of the stimulation and was turned on for the last 20 seconds of the stimulation period. This procedure allowed subjects to feel the sensations (e.g. itching) below the electrodes at the beginning and at the end of the stimulation, making it difficult for naïve subjects to distinguish sham from real stimulation (34). Potential tDCS side effects were assessed with a questionnaire administered immediately at the end of the experimental session. Subjects were required to evaluate intensity of several perceptual sensations (i.e., itching, pain, burning, tingling, discomfort, headache, fatigue, inattention) through a 6-point-scale (i.e., 0 = none, 1 = mild, 2 = moderate, 3 = considerable, 4 = strong, 5 = very strong).

***MRI***

The structural MRI and fMRI scans were performed on a Siemens 3T PET/MRI scanner (with Biograph mMR software VB18P, Siemens, Erlangen, GER). For the resting-state fMRI (rsfMRI), 150 volumes were acquired using a gradient echo-planar-imaging (EPI) sequence with interleaved acquisition. The scan parameters were: TR = 2000 ms, TE = 25 ms, flip angle = 90º, FOV = 24 cm, acquisition matrix = 64 × 64, slice thickness = 4 mm, and 34 axial slices. For the efMRI, 476 volumes were acquired with the same EPI scan parameters as for the rsfMRI. A fieldmap from a double-echo gradient echo sequence was collected for post-scan EPI distortion correction (TR = 1000 ms, TE1 = 3.97 ms, TE2 = 6.43 ms, FOV = 240 mm, slice thickness = 4 mm, design matrix = 64 × 64, flip = 55º). A whole-brain T1-weighted anatomical image was also acquired at the end of the MRI session (about 6 min) using the magnetization prepared rapid gradient echo (MPRAGE) sequence (TR = 3260 ms, TE = 2.26 ms, FOV = 256 mm, slice thickness = 1 mm, design matrix = 256 × 256).

***Experimental design***

Subjects were randomly assigned to the Anodal or Sham groups. Each subject attended two experimental sessions separated by at least 24 hours (Anodal: Mean = 6.6, SD = 6.98 days; Sham: Mean = 7.3, SD = 5.7 days; $t_{(28)} = -.315$ $p = 0.75$) (see Figure 1). In Session 1 (baseline), subjects performed a stop-signal task (Xu et al., 2016) in a quiet testing room without tDCS. They were instructed to stop a response when a visual cue (i.e., a stop-signal) appeared after the response (Go) stimulus onset. The stimulus was either a left or right pointing arrow with a "+" sign in the middle. Subjects were instructed to respond as quickly as possible according to the arrow direction by pressing either the left or the right key on a response box with their right index finger. For 25% of the trials, the "+" sign turned red (i.e., the stop-signal) after the stimulus onset with a short delay (i.e., the stop-signal delay or SSD).

The inter-stimulus-interval (ISI) between trials was jittered with an average about 4 sec (range 2-6 sec). The SSD was dynamically controlled based on whether a successful (Stop) or an unsuccessful (Stop-respond) response was made. The SSD was set at 150 milliseconds (ms) (the shortest SSD) for the first Stop trial, and the longest possible SSD was 450 ms. The SSRT, a measure of the efficiency of response inhibition, was estimated for each participant by subtracting the mean SSD from the $n^{th}$ fastest RT (where n is the percentile corresponding to the probability of the Stop-respond trials) of the primary Go responses (35). The same procedures for estimating the mean of SSD and SSRT were applied to all participants in both groups and sessions. The total length of the stop-signal task was about 15 minutes.

In Session 2, subjects were given two rsfMRI scan runs of 5 minutes each (i.e., pre- and post-tDCS) followed by an efMRI run (15:52 min) during which the subjects performed the stop-signal task identical to that performed during Session 1. About 5 minutes after the end of the first rsfMRI, tDCS (Anodal or Sham) was delivered for 20 minutes outside of the MR scanner. The second rsfMRI scan started about 5 minutes after the tDCS session. The efMRI started immediately after the second rsfMRI scan (about 10 minutes after the end of the tDCS session) (see Figure 1).

***Statistical Analysis***

*Behavioral task*

In all data analyses, Go RTs ≥ two standard deviations of the mean within each subject were considered as "outliers" and were replaced by the mean (average outliers, Session 1: Anodal = 4.4%; Sham = 4.6%; Session 2: Anodal = 4.1%; Sham = 4.3%). RTs ≤ 100 ms were considered as an error response.

The effect of tDCS on response inhibition was estimated by the difference (Δ) of the within-group change in the SSRT between Session 2 and Session 1 (i.e., the ΔSSRT = SSRT [Session 2] – SSRT [Session 1]). This subtraction method effectively normalized each participant's post-tDCS SSRT to his/her pre-tDCS baseline. It also took into account the tendency that SSRT and GoRT tend to be longer in the fMRI scanner environment than in a quiet testing room (36). ΔSSRT allows an estimation of the effect of tDCS on the efficiency of the response inhibition between the Anodal and Sham group, that is, a shorter ΔSSRT indicates more effective inhibitory control in Session 2. The difference in the Go RTs between Session 2 and Session 1 ( GoRT), a measure of the overall response speed, served as a control condition to evaluate whether the effect of tDCS was specific for response stopping. We analysed the effect of anodal tDCS relative to Sham on SSRT and ΔGoRT using two-sample t-tests (2-tailed) (Statistix software version 10 was used to perform the analyses).

***fMRI data processing and analysis***

The rsfMRI and efMRI data were preprocessed using the SPM12 software (the Wellcome Department of Imaging Neuroscience, University College London, UK). All images were EPI distortion corrected with gradient echo EPI fieldmaps collected after the first rsfMRI and after the efMRI. All images within a participant were slice-timing corrected, realigned together, and coregistered with the participant's own high resolution T1 anatomical image. All subjects' T1 images were combined to generate a T1 template using the DARTEL software and procedures, and normalized to the MNI (Montreal Neurological Institute, Canada) template. The normalization parameters from each participant were then applied to the normalization of the participant's own EPI images. The normalized EPI images were smoothed using an 8 × 8 × 8 mm FWHM kernel.

For the rsfMRI runs, the SPM12 preprocessed images were imported into the CONN software (created by MIT: The Gabrieli Lab at the McGovern Institute for Brain Research) (37) and a whole-brain seed-to-voxel based functional connectivity analysis was performed at the second level using the rIFC (pars opercularis) as an a priori seed region of interest (sROI). A binary sROI mask of the rIFC was created in SPM12 using the WFU PickAtlas software (by the Functional MRI Laboratory at the Wake Forest University School of Medicine, NC). The purpose for using the rIFC as a seed ROI was to examine the effect of the Anodal tDCS, relative to the Sham group, on changes in the task-free functional connectivity. The rsfMRI data were de-noised and bandpass filtered at 0.01-0.15 Hz prior to the functional connectivity analysis. The functional connectivity analysis was carried out using the "weighted-GLM" method in CONN and the whole-brain seed-to-voxel analysis at the second level (height threshold $p < 0.001$; extent threshold FDR < 0.05) using the contrasts: 1) Anodal: Post – Pre; and 2) Sham: Post – Pre, looking at within-subject changes in functional connectivity post-tDCS vs Sham.

For the efMRI with the stop-signal task, the preprocessed images were first analyzed with SPM12 software. The first-level design matrix included four response types (Go, Stop, Stop-respond, and error response), Rest, and six motion parameters. The efMRI activation was modeled using the canonical hemodynamic response function (HRF) with temporal and dispersion derivatives. The data were high-pass filtered at 128 sec and the event duration for response types was set at 1 sec and for Rest 9 sec. The Rest period served as a baseline for all contrasts with response types. Contrasts from first-level analysis were fed into the second-level group analysis using two-sample t tests and the "flexible factorial" design option with a main effect of Subject and an interaction term (i.e., Group [Anodal vs Sham] × Response

[Stop vs Go]). In addition, ROI-to-ROI functional connectivity analyses were carried out using the CONN software with the generalized Psycho-Physiological Interaction (gPPI) (37) focusing on three critical links in the fronto-basal-ganglia network: the rPreSMA – rIFC, rPreSMA – STN, and rIFC - STN. The ROI-to-ROI analyses were carried out with the contrast: Anodal – Sham. The locus of the rPreSMA ROI (xyz = 10, 10, 60; 6 mm radius) was based on a recent TMS-fMRI study demonstrating its connectivity within the fronto-basal-ganglia network (38). The rIFC and STN ROIs were extracted using the WFU PickAtlas software (by the Functional MRI Laboratory at the Wake Forest University School of Medicine, NC) with the Automated Anatomical Labelling toolbox. All fMRI activation results were significant based on voxel-wise analyses corrected for multiple comparisons (FDR $p < 0.05$).

## Results

*Sensations related to tDCS*

The sensations scores reported by the Anodal group were similar to the sensations scores reported by the Sham group (Anodal group: mean = 1.3, SD = 1.9, Sham group: mean = 1.22, SD = 1.9; Z = 0.28, p = 0.77).

***Behavioral results***

On average, the subjects made 50.4% (SD ± 6.35) of stop responses (i.e., successfully stopped responses) in Session 1: Anodal group = 48.4% (SD ± 2.8); Sham group: 51.8% (SD ± 7.81); and 46.84% (SD ± 5.94) of stop responses in Session 2: Anodal group = 47.5% (SD ± 5.34); Sham group = 46.5% (SD ± 6.4). Regarding the baseline (Session 1) performance, two-sample t-test (2-tailed) showed no significant differences in SSRT and GoRT between

the Anodal and Sham groups (SSRT: $t_{(28)} = 1.15$, $p = 0.25$; Go RTs: $t_{(28)} = -1.20$, $p = 0.24$) (see Table 1).

Planned t-tests (2-tailed) on the difference scores of response time between Session 2 and Session 1 (i.e. the SSRT and GoRT) showed a significant difference between the Anodal and Sham tDCS groups ( SSRT: $t_{(28)} = -2.29$, $p = 0.03$), with shorter SSRT (indicating better inhibitory performance) for the Anodal group (40 ms [± 27]) post-tDCS compared to the Sham group (65 ms [± 33]) (Figure 2a-b). In addition, no significant differences were observed between groups with the GoRT (Anodal group = 25 ms [± 28]; Sham group = 21 ms [± 70]; $t_{(28)} = 0.20$, $p = 0.84$) (see Figure 2a). Anodal tDCS improved SSRT but not the overall response speed measured by GoRT. This finding suggests behavioral specificity for response inhibition (Logan, 1994).

The fact that SSRT and GoRT in session 2 (inside the MRI scanner) were prolonged compared to those in Session 1 (quiet testing room) is consistent with previous findings (36). The authors reported that when participants performed a perceptual decision-making task both in a regular laboratory setting as well as inside the fMRI scanner, the results consistently showed that response times increased inside the scanner (36).

---

Insert Table 1 about here

---

---

Insert Figure 2 about here

---

306 ***fMRI results***

307 rsfMRI. The results of the whole-brain rsfMRI functional connectivity analysis using the
308 rIFC as the Seed ROI revealed a significant increase (voxel-level threshold $p < .001$; FDR $p <$
309 .05) in the functional connectivity post-tDCS between the rIFC and the caudate (left: xyz = -
310 16, -3, 20; right: xyz = 20, -4, 18). This increase in connectivity was only observed in the
311 Anodal tDCS group (Figure 3).

312 ----------

313 Insert Figure 3 about here

314 ----------

315 efMRI. The efMRI whole-brain analysis showed similar patterns of brain activation during
316 the Go and Stop responses in both the Anodal and Sham groups (Figure 4). The patterns of
317 activation were consistent with previous findings using stop-signal tasks (12, 39, 40). For
318 both the Anodal and Sham group, Go responses activated primarily the left M1 and
319 cerebellum, while Stop responses induced significant activation in the rIFC and the basal-
320 ganglia. There were no statistically significant differences observed between groups in BOLD
321 signals. These results indicate that tDCS with the anode over the rIFC in this study did not
322 significantly alter globally the functioning of the fronto-basal-ganglia network during the
323 primary Go and Stop responses.

324 ----------

325 Insert Figure 4 about here

326 ----------

327 However, results of the functional connectivity analysis using a priori regions of interest
328 (ROI)-to-ROI focusing on the three critical links in the fronto-basal ganglia network: the
329 rPreSMA – rIFC, the rPreSMA – STN, and rIFC – STN showed a significant increase in
330 connectivity between the rPreSMA and STN (voxel threshold $p < 0.001$; cluster FDR $< 0.05$)

in the Anodal group (0.11 [± 0.04]) during the Stop responses relative to that in the Sham group (- 0.03 [± 03]) ($t_{(28)}$ = 2.87, p = 0.01) (Figure 5). No statistically significant changes in functional connectivity were observed during the Go responses.

---

Insert Figure 5 about here

---

To further examine the tDCS effect on brain activation and its relation to the SSRT and rsfMRI connectivity as an exploratory step**,** BOLD signal values (i.e., first eigenvalues of clusters) that showed significant (FDR < 0.05) differences between Stop and Go responses across the Anodal and Sham groups were extracted. The eigenvalues of the significant clusters were extracted by applying a binary ROI mask that included only regions showing an interaction in rsfMRI functional connectivity (i.e., [Anodal - Sham] - [Stop - Go]; see Figure 6a) using a seed [rIFC] to whole-brain functional connectivity analysis. The ROI analysis resulted in three significant clusters/regions: rPreSMA (xyz = 11, 27, 39), rIPC (xyz = 43, -54, 42), and rDLPFC (xyz = 43, 27, 36). A mixed repeated measures ANOVA (mRANOVA) including all three regions showed a significant main effect of Group ($F_{(1,28)}$ = 5.59, MSe = 1.729, p = 0.025) and Group by Region interaction ($F_{(1,28)}$ = 3.32, MSe = 0.433, p = 0.043) during the Stop responses. No significant differences were observed in Go responses. Separate two-sample t-tests (2-tailed) showed that the BOLD activation in the rIPC and rDLPFC were significantly lower in the Anodal than the Sham group (rIPC: $t_{(1,28)}$ = -2.02, p = 0.05; rDLPFC: $t_{(1,28)}$ = -2.73, p = 0.01) (Figure 6b).

---

Insert Figure 6 about here

---

To examine the relationship between the effects of tDCS on brain activity in these regions and the efficiency of response inhibition, all three regions were entered in two separate multiple linear regression models for the Anodal and Sham group with the SSRT from the efMRI session as the dependent variable. The two regression models included either the three clusters with the BOLD signals from the Stop responses as the predictor variables or those from the Go responses as the predictor variables. The results showed that for the Anodal tDCS group, only BOLD activation during the Go responses in the rIPC and rDLPFC was predictive of SSRT (Table 2a). Similar regression results were not observed for the Sham group. The regression coefficients of determination ($R^2$) associated with the rIPC and rDLPFC accounted for 74% (partial $R^2$: rIPC = 0.34; rDLPFC = 0.40) of the variance in the SSRT of the Anodal group. However, the regression analyses of the Sham condition showed that the BOLD signal in the rPreSMA and rIPC during the Stop responses were predictive of the SSRT (Table 2b). This is not surprising for the Sham condition as the rPreSMA, in particular, has been shown to be a critical node for rapid response inhibition (12, 16, 41-43).

---

Insert Table 2 about here

---

**Discussion**

Consistent with the findings of previous tDCS studies that used the same cephalic montage (17-19), tDCS with the anode over the rIFC facilitated response inhibition relative to Sham tDCS. More importantly, the behavioral effect was specific to the speed of inhibition ( SSRT) and not general to all responses ( GoRT).

The brain activation and connectivity results further indicated that anodal tDCS induced significant changes in the neural dynamics of functional connectivity between the targeted rIFC and subcortical regions (e.g., caudate) as well as brain activity in other regions (e.g., rDLPFC and rIPC). These observations are consistent with previous studies that have also reported the involvement of the dorsolateral prefrontal cortex (DLPFC) and inferior parietal cortex (IPC) (44-46). Dynamic changes in brain activity induced by anodal tDCS strengthened the functional connectivity between the rPreSMA and STN, the hyperdirect pathway of the fronto-basal ganglia network mediating rapid response inhibition (7, 12, 47).

These results suggest that tDCS with the anode over the rIFC induces dynamic neural modulation in the rIFC, rDLPFC, rPreSMA, basal ganglia, and their interconnected brain regions (e.g., rIPC). This dynamic neural modulation is likely to influence not only spontaneous brain activity but also the strength of functional connectivity between interconnected network nodes, which in turn, enhances information processing efficiency and network synchronization (e.g., rPreSMA – STN) critical to achieving rapid response inhibition. The specificity of the tDCS effect with the anode positioned over rIFC on response inhibition is likely, in part, due to the presence of direct white matter connections between the rIFC, the rPreSMA, and the basal ganglia (48-51). There is evidence that the efficiency of response inhibition (i.e. SSRT) correlates with the microstructural white-matter properties of these tracts (e.g., fractional anisotropy, fiber length, and mean diffusivity) (38, 50, 52, 53). However, it should be pointed out that, due to the electrode montage employed in our study and the non-focal nature of tDCS, we cannot rule out that the observed results reflect a combined effect of stimulation of the rIFC and other regions of the frontal cortex such as the frontopolar region.

The rsfMRI results further indicated that anodal tDCS strengthened the intrinsic/spontaneous functional connectivity between the rIFC and caudate, a part of the fronto-basal-ganglia network engaged in rapid stopping responses (7, 12). These changes in spontaneous brain activation patterns and connectivity strength within the fronto-basal-ganglia network likely contributed to the efficiency in performing the task during efMRI. As the results showed, the anodal tDCS significantly increased the strength of the functional connectivity during Stop responses between the rPreSMA and STN, a critical pathway for rapid stopping responses (12). In addition, the results of the study suggest that changes in functional connectivity may be coupled with changes in task-related brain activity consequential to specific cognitive processes, in this case, response inhibition. This is evidenced by the effects of the tDCS on the rsfMRI functional connectivity that were, to some extent, coincided with the BOLD signal change in the rDLPFC and rIPC during Stop responses (Figure 6), and that activity in these brain regions during Go responses was predictive of the efficiency of stopping.

Previous tDCS-fMRI studies reported that anodal tDCS was able to increase cortical excitability and enhance behavioral performance by reducing brain activity and modulating functional or effective connectivity (54-57). Findings in a recent study combining tDCS with large-scale neurophysiological recordings from monkeys were consistent with the observation that tDCS induces functional change by dynamic modulation of functional connectivity (58). Clearly, anodal tDCS affected not just the functioning of the fronto-basal-ganglia network critical to the stopping response. Results from both our rsfMRI and efMRI showed some evidence of modification in brain activity and functional connectivity in the fronto-parietal regions including the rDLPFC and rIPC.

A previous analysis (59) of 70 published inhibitory control studies also showed that rIFC had

stronger intrinsic and task-evoked functional connectivity with key nodes of the fronto-parietal network, including DLPFC and IPC. Some evidence suggests that this network may play a role in maintaining task-relevant information for rapid adjustment of response control (60). Although the exact role of these regions in rapid response inhibition remains to be determined, previous findings suggest that the rDLPFC and the posterior parietal cortex may be engaged in rapid response inhibition via an enhanced preparatory or goal-directed process (44-46, 61-63). Our results showed that the BOLD activation in the rDLPFC and rIPC during the Go responses accounted for 74% of the variance in the SSRT (Table 2a). This is consistent with previous observations that preparatory process or proactive control facilitates response inhibition and shortens the SSRT (64). It is possible that rDLPFC and rIPC facilitated rapid stopping responses by modulating the response tendency (12). The occasional occurrence of the Stop signal in the task induces the proactive control of sustained attention on the Go process in order to maintain task goals (i.e., to avoid responding too quickly that it becomes difficult to withhold a response when the Stop signal is detected) (45, 65, 66). Evidence from intracranial electroencephalography (44) revealed that activity in the rDLPFC occurred around the presentation of a task cue and/or the Go cue, while activity in the rIFC was present more consistently after the Go cue prior to the motor response. These different temporal profiles suggest that the rDLPFC may be engaged in task goals while rIFC implements action control (44). The current results further demonstrate that both the rDLPFC and rIPC are an integral part of the fronto-basal-ganglia network critical for rapid response inhibition. Understanding how the tDCS affects brain activity and network functional connectivity as well as task related mechanisms underlying the facilitatory effect on response inhibition provides the potential for developing non-invasive brain stimulation interventions to improve this critical cognitive function in patients with deficits in the fronto-basal ganglia inhibitory control circuits. Future studies may overcome potential limitations of the current

455 design by considering a within-subject design and better stimulation controls, and, if possible,
456 delivering tDCS with task performance inside the scanner.
457
458 **Conclusions**

This study shows for the first time that tDCS with the anode over the rIFC and the cathode over the left supraorbital region facilitates response inhibition by modulating brain activity and functional connectivity in the fronto-basal-ganglia network. In addition, the results of the efMRI support the observation that the rDLPFC and rIPC are an integral component of the response inhibition network.

**Acknowledgments:**

This work was supported by the United States Department of Defense through the Center for Neuroscience and Regenerative Medicine (G189BK) and by the Intramural Research Program of the National Institute of Neurological Disorders and Stroke, at the National Institutes of Health. We thank Dr. Gang Chen at the National Institute of Mental Health for his input on data analysis.
459

## References


1.Logan GD, Cowan WB. On the Ability to Inhibit Thought and Action - a Theory of an Act of Control. Psychological Review. 1984;91(3):295-327.

2.Miyake A, Friedman NP. The Nature and Organization of Individual Differences in Executive Functions: Four General Conclusions. Curr Dir Psychol Sci. 2012;21(1):8-14.

3.Aron AR, Fletcher PC, Bullmore ET, Sahakian BJ, Robbins TW. Stop-signal inhibition disrupted by damage to right inferior frontal gyrus in humans. Nat Neurosci. 2003;6(2):115-6.

4.Sumner P, Nachev P, Morris P, Peters AM, Jackson SR, Kennard C, et al. Human medial frontal cortex mediates unconscious inhibition of voluntary action. Neuron. 2007;54(5):697-711.

5.Nachev P, Kennard C, Husain M. Functional role of the supplementary and pre-supplementary motor areas. Nat Rev Neurosci. 2008;9(11):856-69.

6.Sebastian A, Gerdes B, Feige B, Kloppel S, Lange T, Philipsen A, et al. Neural correlates of interference inhibition, action withholding and action cancelation in adult ADHD. Psychiatry Res. 2012;202(2):132-41.

7.Jahanshahi M, Obeso I, Rothwell JC, Obeso JA. A fronto-striato-subthalamic-pallidal network for goal-directed and habitual inhibition. Nat Rev Neurosci. 2015;16(12):719-32.

8.Dalley JW, Robbins TW. Fractionating impulsivity: neuropsychiatric implications. Nat Rev Neurosci. 2017;18(3):158-71.

9.Xu B, Sandrini M, Levy S, Volochayev R, Awosika O, Butman JA, et al. Lasting deficit in inhibitory control with mild traumatic brain injury. Scientific Reports. 2017;7(1):14902.

10.Logan GD, Cowan WB, Davis KA. On the ability to inhibit simple and choice reaction time responses: a model and a method. J Exp Psychol Hum Percept Perform. 1984;10(2):276-91.

11.Verbruggen F, Logan GD. Models of response inhibition in the stop-signal and stop-change paradigms. Neurosci Biobehav Rev. 2008;33(5):647-61.

12.Aron AR. From reactive to proactive and selective control: developing a richer model for stopping inappropriate responses. Biol Psychiatry. 2011;69(12):e55-68.

13.Aron AR, Robbins TW, Poldrack RA. Inhibition and the right inferior frontal cortex: one decade on. Trends Cogn Sci. 2014;18(4):177-85.

14.Chambers CD, Bellgrove MA, Gould IC, English T, Garavan H, McNaught E, et al. Dissociable mechanisms of cognitive control in prefrontal and premotor cortex. J Neurophysiol. 2007;98(6):3638-47.

15.Verbruggen F, Aron AR, Stevens MA, Chambers CD. Theta burst stimulation dissociates attention and action updating in human inferior frontal cortex. Proc Natl Acad Sci U S A. 2010;107(31):13966-71.

16.Lee HW, Lu MS, Chen CY, Muggleton NG, Hsu TY, Juan CH. Roles of the pre-SMA and rIFG in conditional stopping revealed by transcranial magnetic stimulation. Behav Brain Res. 2016;296:459-67.

17.Jacobson L, Javitt DC, Lavidor M. Activation of inhibition: diminishing impulsive behavior by direct current stimulation over the inferior frontal gyrus. Journal of Cognitive Neuroscience. 2011;23(11):3380-7.

18.Ditye T, Jacobson L, Walsh V, Lavidor M. Modulating behavioral inhibition by tDCS combined with cognitive training. Exp Brain Res. 2012;219(3):363-8.

19.Stramaccia DF, Penolazzi B, Sartori G, Braga M, Mondini S, Galfano G. Assessing the effects of tDCS over a delayed response inhibition task by targeting the right inferior frontal gyrus and right dorsolateral prefrontal cortex. Exp Brain Res. 2015;233(8):2283-90.

509 20.Hogeveen J, Grafman J, Aboseria M, David A, Bikson M, Hauner KK. Effects of
510 High-Definition and Conventional tDCS on Response Inhibition. Brain Stimul.
511 2016;9(5):720-9.
512 21.Zandbelt BB, Bloemendaal M, Hoogendam JM, Kahn RS, Vink M. Transcranial
513 magnetic stimulation and functional MRI reveal cortical and subcortical interactions during
514 stop-signal response inhibition. J Cogn Neurosci. 2013;25(2):157-74.
515 22.Watanabe T, Hanajima R, Shirota Y, Tsutsumi R, Shimizu T, Hayashi T, et al. Effects
516 of rTMS of Pre-Supplementary Motor Area on Fronto Basal Ganglia Network Activity
517 during Stop-Signal Task. J Neurosci. 2015;35(12):4813-23.
518 23.Saiote C, Turi Z, Paulus W, Antal A. Combining functional magnetic resonance
519 imaging with transcranial electrical stimulation. Frontiers in human neuroscience.
520 2013;7:435.
521 24.Venkatakrishnan A, Sandrini M. Combining transcranial direct current stimulation
522 and neuroimaging: novel insights in understanding neuroplasticity. J Neurophysiol.
523 2012;107(1):1-4.
524 25.Yu J, Tseng P, Hung DL, Wu SW, Juan CH. Brain stimulation improves cognitive
525 control by modulating medial-frontal activity and preSMA-vmPFC functional connectivity.
526 Hum Brain Mapp. 2015;36(10):4004-15.
527 26.Hsu TY, Tseng LY, Yu JX, Kuo WJ, Hung DL, Tzeng OJ, et al. Modulating
528 inhibitory control with direct current stimulation of the superior medial frontal cortex.
529 Neuroimage. 2011;56(4):2249-57.
530 27.Friston KJ. Functional and effective connectivity: a review. Brain connectivity.
531 2011;1(1):13-36.
532 28.Oldfield RC. The assessment and analysis of handedness: the Edinburgh inventory.
533 Neuropsychologia. 1971;9(1):97-113.
534 29.Dayan E, Censor N, Buch ER, Sandrini M, Cohen LG. Noninvasive brain stimulation:
535 from physiology to network dynamics and back. Nat Neurosci. 2013;16(7):838-44.
536 30.Nitsche MA, Cohen LG, Wassermann EM, Priori A, Lang N, Antal A, et al.
537 Transcranial direct current stimulation: State of the art 2008. Brain Stimul. 2008;1(3):206-23.
538 31.Jacobson L, Koslowsky M, Lavidor M. tDCS polarity effects in motor and cognitive
539 domains: a meta-analytical review. Exp Brain Res. 2012;216(1):1-10.
540 32.Antal A, Alekseichuk I, Bikson M, Brockmoller J, Brunoni AR, Chen R, et al. Low
541 intensity transcranial electric stimulation: Safety, ethical, legal regulatory and application
542 guidelines. Clin Neurophysiol. 2017;128(9):1774-809.
543 33.Levy BJ, Wagner AD. Cognitive control and right ventrolateral prefrontal cortex:
544 reflexive reorienting, motor inhibition, and action updating. Ann N Y Acad Sci.
545 2011;1224:40-62.
546 34.Gandiga PC, Hummel FC, Cohen LG. Transcranial DC stimulation (tDCS): a tool for
547 double-blind sham-controlled clinical studies in brain stimulation. Clin Neurophysiol.
548 2006;117(4):845-50.
549 35.Logan GD. On the ability to inhibit thought and action: A user's guide to the stop
550 signal paradigm. In: Dagenbach D, Carr TH, editors. Inhibitory Processes in Attention,
551 Memory and Language. San Diego: Academic; 1994. p. 189-239.
552 36.van Maanen L, Forstmann BU, Keuken MC, Wagenmakers EJ, Heathcote A. The
553 impact of MRI scanner environment on perceptual decision-making. Behav Res Methods.
554 2016;48(1):184-200.
555 37.Whitfield-Gabrieli S, Nieto-Castanon A. Conn: a functional connectivity toolbox for
556 correlated and anticorrelated brain networks. Brain connectivity. 2012;2(3):125-41.

38.Xu B, Sandrini M, Wang WT, Smith JF, Sarlls JE, Awosika O, et al. PreSMA stimulation changes task-free functional connectivity in the fronto-basal-ganglia that correlates with response inhibition efficiency. Hum Brain Mapp. 2016;37(9):3236-49.
39.Aron AR, Poldrack RA. Cortical and subcortical contributions to Stop signal response inhibition: role of the subthalamic nucleus. J Neurosci. 2006;26(9):2424-33.
40.Xu B, Levy S, Butman J, Pham D, Cohen LG, Sandrini M. Effect of foreknowledge on neural activity of primary "go" responses relates to response stopping and switching. Frontiers in human neuroscience. 2015;9:34.
41.Chen CY, Muggleton NG, Tzeng OJ, Hung DL, Juan CH. Control of prepotent responses by the superior medial frontal cortex. Neuroimage. 2009;44(2):537-45.
42.Cai W, George JS, Verbruggen F, Chambers CD, Aron AR. The role of the right presupplementary motor area in stopping action: two studies with event-related transcranial magnetic stimulation. J Neurophysiol. 2012;108(2):380-9.
43.Obeso I, Robles N, Marron EM, Redolar-Ripoll D. Dissociating the Role of the pre-SMA in Response Inhibition and Switching: A Combined Online and Offline TMS Approach. Frontiers in human neuroscience. 2013;7:150.
44.Swann NC, Tandon N, Pieters TA, Aron AR. Intracranial electroencephalography reveals different temporal profiles for dorsal- and ventro-lateral prefrontal cortex in preparing to stop action. Cereb Cortex. 2013;23(10):2479-88.
45.Hughes ME, Budd TW, Fulham WR, Lancaster S, Woods W, Rossell SL, et al. Sustained brain activation supporting stop-signal task performance. Eur J Neurosci. 2014;39(8):1363-9.
46.van Belle J, Vink M, Durston S, Zandbelt BB. Common and unique neural networks for proactive and reactive response inhibition revealed by independent component analysis of functional MRI data. Neuroimage. 2014;103:65-74.
47.Chambers CD, Garavan H, Bellgrove MA. Insights into the neural basis of response inhibition from cognitive and clinical neuroscience. Neurosci Biobehav Rev. 2009;33(5):631-46.
48.Akkal D, Dum RP, Strick PL. Supplementary motor area and presupplementary motor area: targets of basal ganglia and cerebellar output. J Neurosci. 2007;27(40):10659-73.
49.Catani M, Dell'acqua F, Vergani F, Malik F, Hodge H, Roy P, et al. Short frontal lobe connections of the human brain. Cortex. 2012;48(2):273-91.
50.King AV, Linke J, Gass A, Hennerici MG, Tost H, Poupon C, et al. Microstructure of a three-way anatomical network predicts individual differences in response inhibition: a tractography study. Neuroimage. 2012;59(2):1949-59.
51.Aron AR, Herz DM, Brown P, Forstmann BU, Zaghloul K. Frontosubthalamic Circuits for Control of Action and Cognition. J Neurosci. 2016;36(45):11489-95.
52.Forstmann BU, Keuken MC, Jahfari S, Bazin PL, Neumann J, Schafer A, et al. Cortico-subthalamic white matter tract strength predicts interindividual efficacy in stopping a motor response. Neuroimage. 2012;60(1):370-5.
53.Rae CL, Hughes LE, Anderson MC, Rowe JB. The prefrontal cortex achieves inhibitory control by facilitating subcortical motor pathway connectivity. J Neurosci. 2015;35(2):786-94.
54.Antal A, Polania R, Schmidt-Samoa C, Dechent P, Paulus W. Transcranial direct current stimulation over the primary motor cortex during fMRI. Neuroimage. 2011;55(2):590-6.
55.Holland R, Leff AP, Josephs O, Galea JM, Desikan M, Price CJ, et al. Speech facilitation by left inferior frontal cortex stimulation. Curr Biol. 2011;21(16):1403-7.
56.Holland R, Leff AP, Penny WD, Rothwell JC, Crinion J. Modulation of frontal effective connectivity during speech. Neuroimage. 2016;140:126-33.

57.Meinzer M, Antonenko D, Lindenberg R, Hetzer S, Ulm L, Avirame K, et al. Electrical brain stimulation improves cognitive performance by modulating functional connectivity and task-specific activation. J Neurosci. 2012;32(5):1859-66.
58.Krause MR, Zanos TP, Csorba BA, Pilly PK, Choe J, Phillips ME, et al. Transcranial Direct Current Stimulation Facilitates Associative Learning and Alters Functional Connectivity in the Primate Brain. Curr Biol. 2017;27(20):3086-96 e3.
59.Cai W, Ryali S, Chen T, Li CS, Menon V. Dissociable roles of right inferior frontal cortex and anterior insula in inhibitory control: evidence from intrinsic and task-related functional parcellation, connectivity, and response profile analyses across multiple datasets. J Neurosci. 2014;34(44):14652-67.
60.Dosenbach NU, Fair DA, Cohen AL, Schlaggar BL, Petersen SE. A dual-networks architecture of top-down control. Trends Cogn Sci. 2008;12(3):99-105.
61.Coulthard EJ, Nachev P, Husain M. Control over conflict during movement preparation: role of posterior parietal cortex. Neuron. 2008;58(1):144-57.
62.Cieslik EC, Zilles K, Caspers S, Roski C, Kellermann TS, Jakobs O, et al. Is there "one" DLPFC in cognitive action control? Evidence for heterogeneity from co-activation-based parcellation. Cereb Cortex. 2013;23(11):2677-89.
63.Smittenaar P, Guitart-Masip M, Lutti A, Dolan RJ. Preparing for selective inhibition within frontostriatal loops. J Neurosci. 2013;33(46):18087-97.
64.Chikazoe J, Jimura K, Asari T, Yamashita K, Morimoto H, Hirose S, et al. Functional dissociation in right inferior frontal cortex during performance of go/no-go task. Cereb Cortex. 2009;19(1):146-52.
65.Braver TS, Barch DM. Extracting core components of cognitive control. Trends Cogn Sci. 2006;10(12):529-32.
66.Forster S, Nunez Elizalde AO, Castle E, Bishop SJ. Unraveling the anxious mind: anxiety, worry, and frontal engagement in sustained attention versus off-task processing. Cereb Cortex. 2015;25(3):609-18.

649 **Figure Captions:**

650 **Figure 1.** Figure 1 shows the schematic illustration of the experimental procedure. Subjects
651 performed the stop-signal task without tDCS in a testing room during Session 1 (baseline). In
652 Session 2 (at least 24 hours after Session 1), resting-state fMRI (rsfMRI) data were acquired
653 before and after tDCS (real or sham) with the anode over the rIFC. tDCS was applied outside
654 of the MR scanner using a bipolar montage with the cathode placed over the left supraorbital
655 area. Immediately after the second rsfMRI scan, the participants performed the stop-signal
656 task again during the fMRI scan.

657

658 **Figure 2.** Figure 2a shows the tDCS effects on behavioral responses. Note shortening of delta
659 SSRT in the anodal tDCS group relative to the Sham group using two-tailed two-sample t-
660 tests.
661 Figure 2b shows the individual SSRTs of Anodal and Sham groups in Session 1 (baseline)
662 and Session 2.

663

664 **Figure 3**. Figure 3 shows the rsfMRI activation clusters in the T1 sagittal MRI images that
665 had the significant increase (voxel-level threshold $p < .001$; FDR $p < .05$) in functional
666 connectivity post-tDCS between rIFC and left and right caudate in the Anodal group (i.e.,
667 post-tDCS – pre-tDCS). The bar graph shows the mean increases (Fisher's Z scores) in the
668 strength of the functional connectivity post-tDCS.

669

**Figure 4.** Figure 4 shows brain activation patterns of Go and Stop responses in the Anodal and Sham groups post-tDCS (corrected for multiple comparisons FDR < 0.05, cluster Ext = 50). There were no significant statistical differences in the BOLD signal between groups using whole brain voxel-wise analyses. Cereb = cerebellum, M1 = primary motor cortex, STN = subthalamic nucleus, rPreSMA = right pre-supplementary motor area, rIPC = right inferior parietal cortex.

**Figure 5.** Figure 5 shows the significant increase (voxel-level threshold $p < .001$; FDR $p < .05$) in the efMRI functional connectivity (gPPI) between rPreSMA and STN during the Stop responses after anodal tDCS relative to the Sham condition.

**Figure 6.** Figure 6a: rsfMRI showing an interaction ($p < 0.01$ uncorrected, FDR < 0.05) between Group (Anodal – Sham) x Session (Post – Pre) in the two large clusters (xyz = 18, 16, 38; xyz = 33, -51, 36) that included rDLPFC, rPreSMA, and rIPC. The connectivity values (Fisher's Z) showed a decrease in connectivity post-tDCS (rDLPFC = -0.081; rIPC = -0.11) in the Anodal group relative to the Sham group (rDLPFC = 0.1; rIPC = 0.088). 6b shows that similar regions in efMRI had reduced BOLD activation in the Anodal group relative to Sham in rIPC and rDLPFC.

**Figure 1**

Click here to download high resolution image

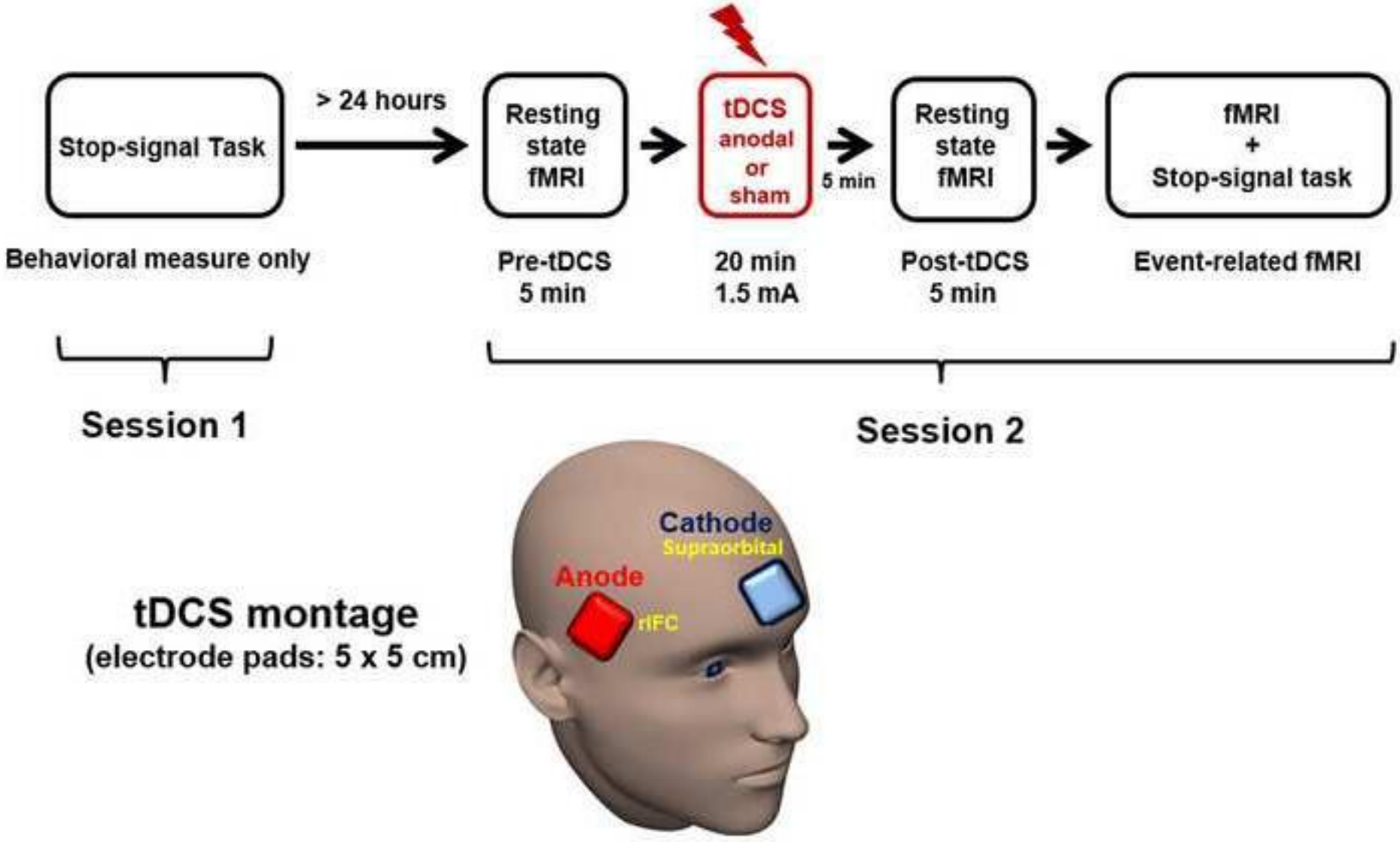

Figure 2

Click here to download high resolution image

a.

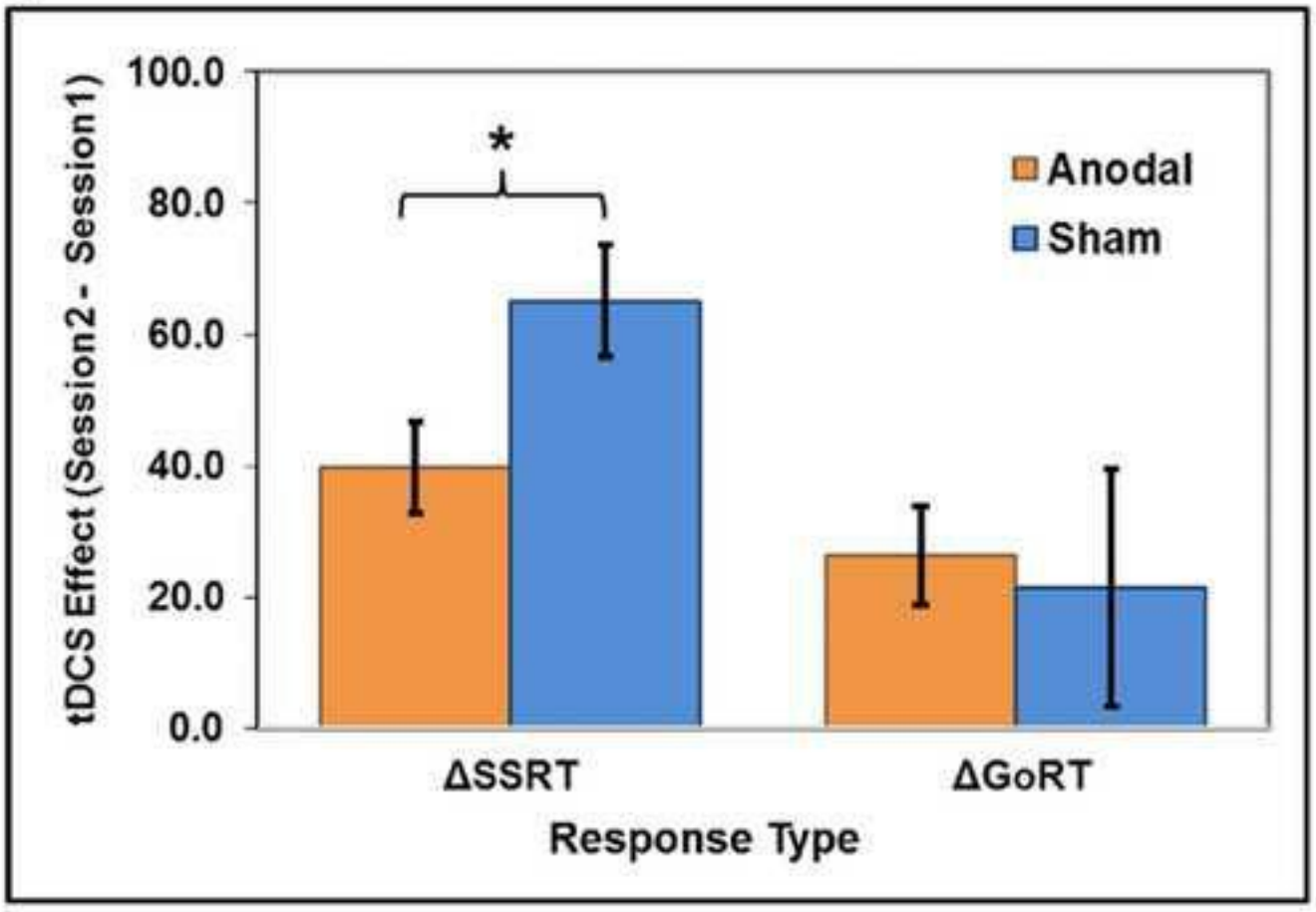


b.

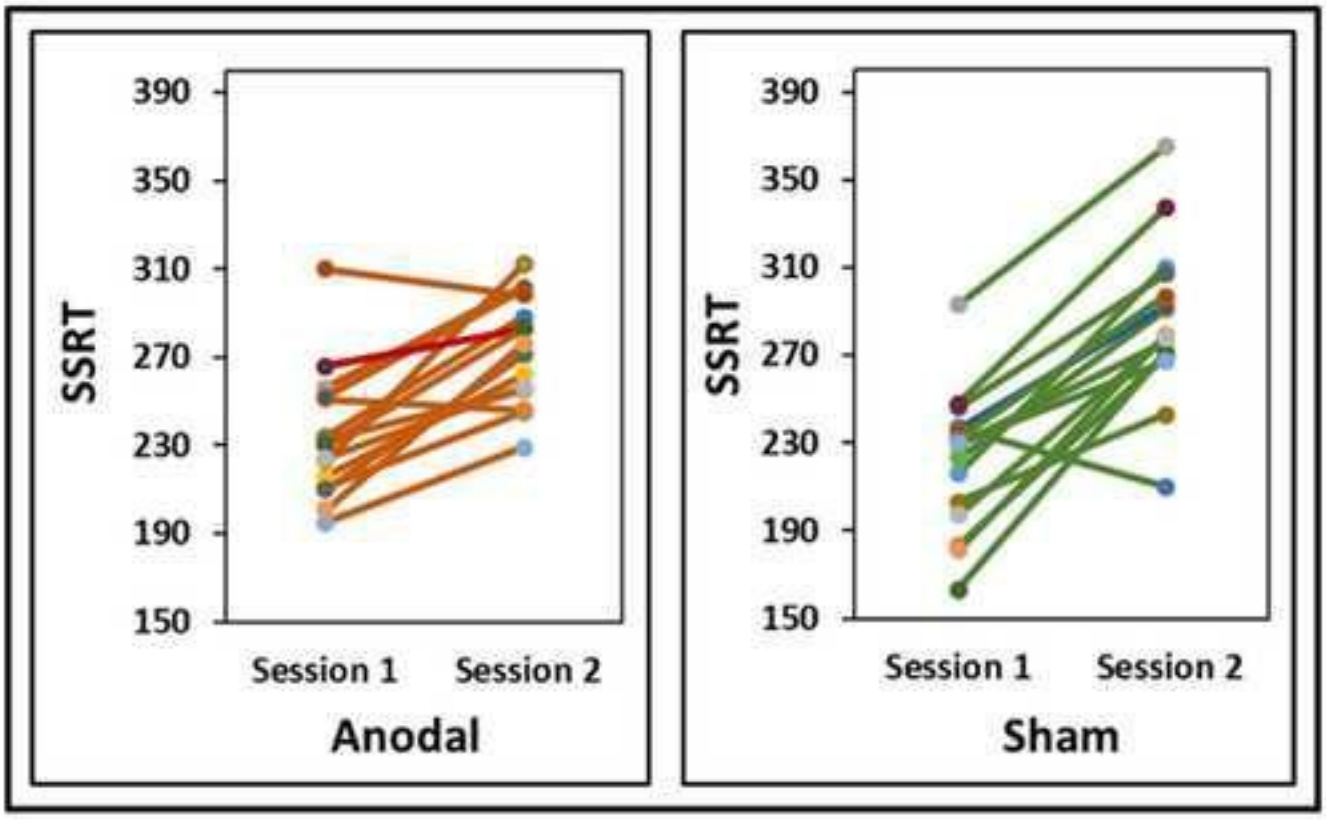

**Figure 3**

Click here to download high resolution image

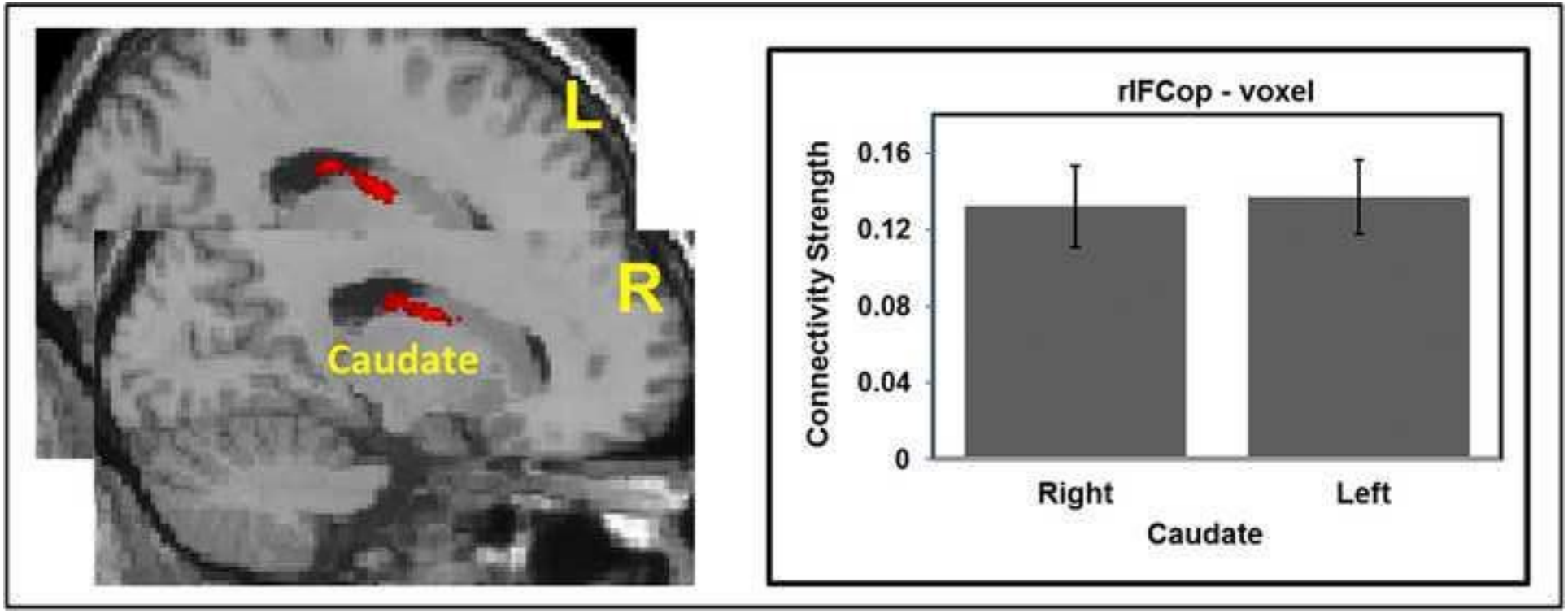

**Figure 4**

Click here to download high resolution image

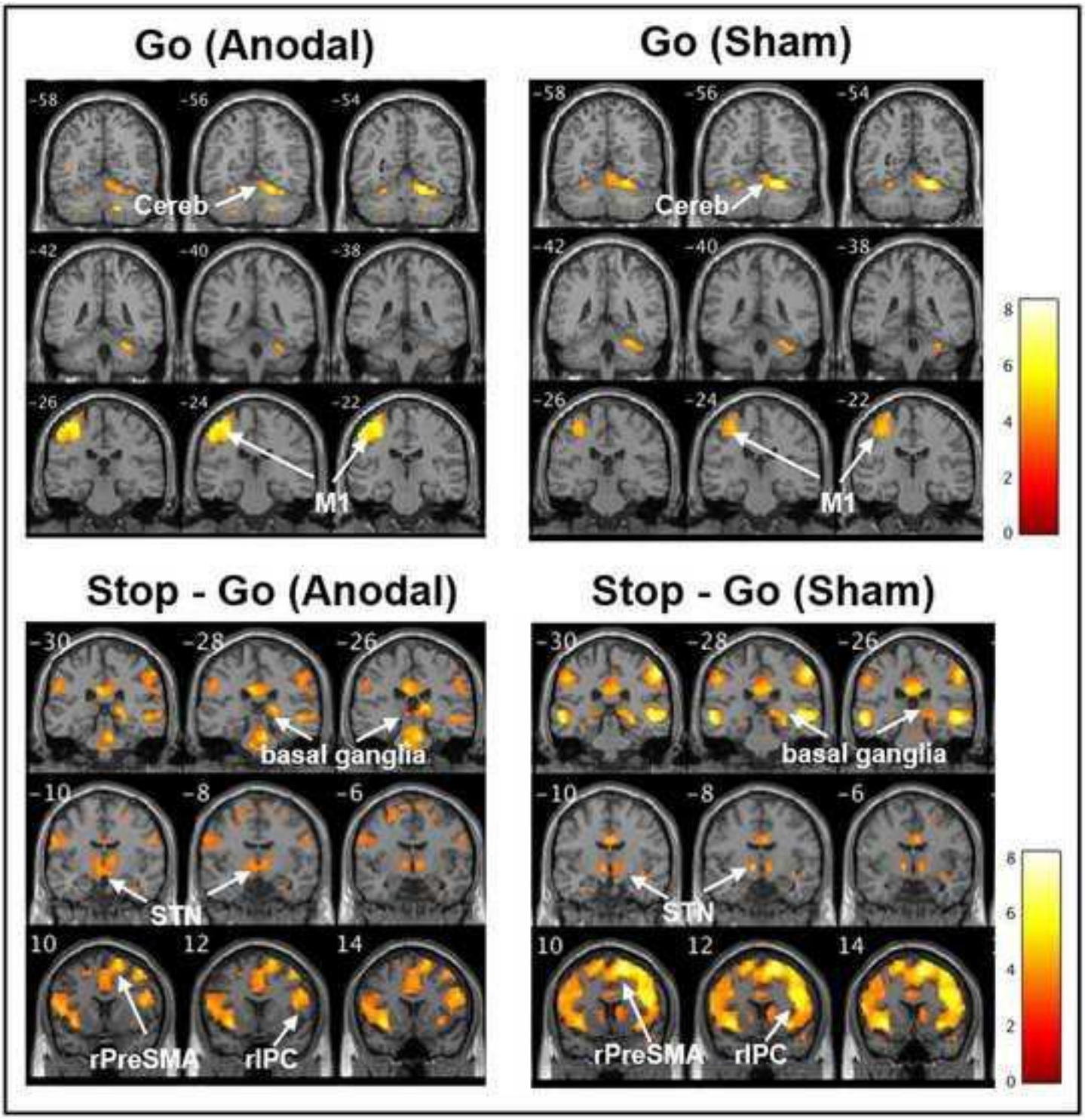

Figure 5

Click here to download high resolution image

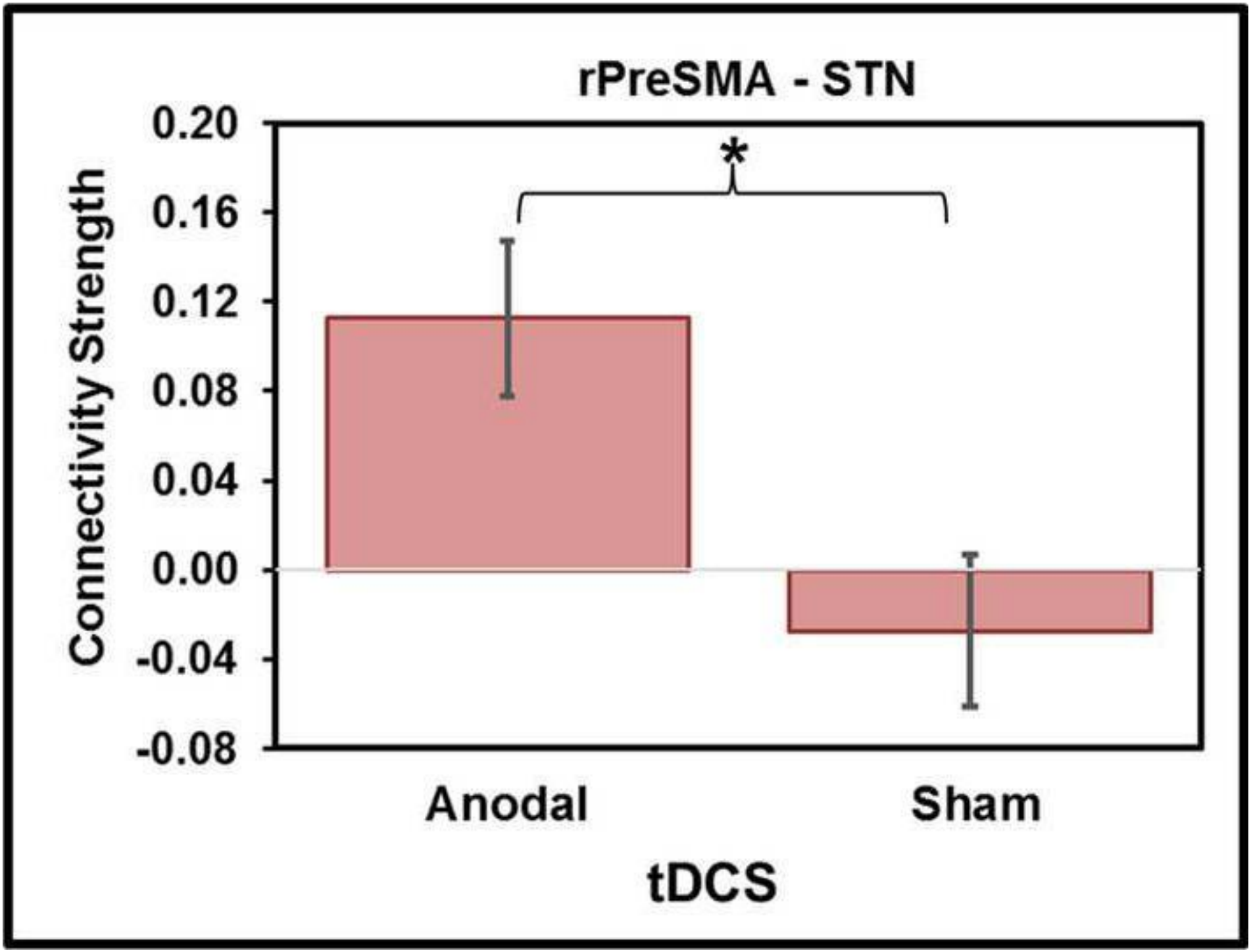

**Figure 6**

Click here to download high resolution image

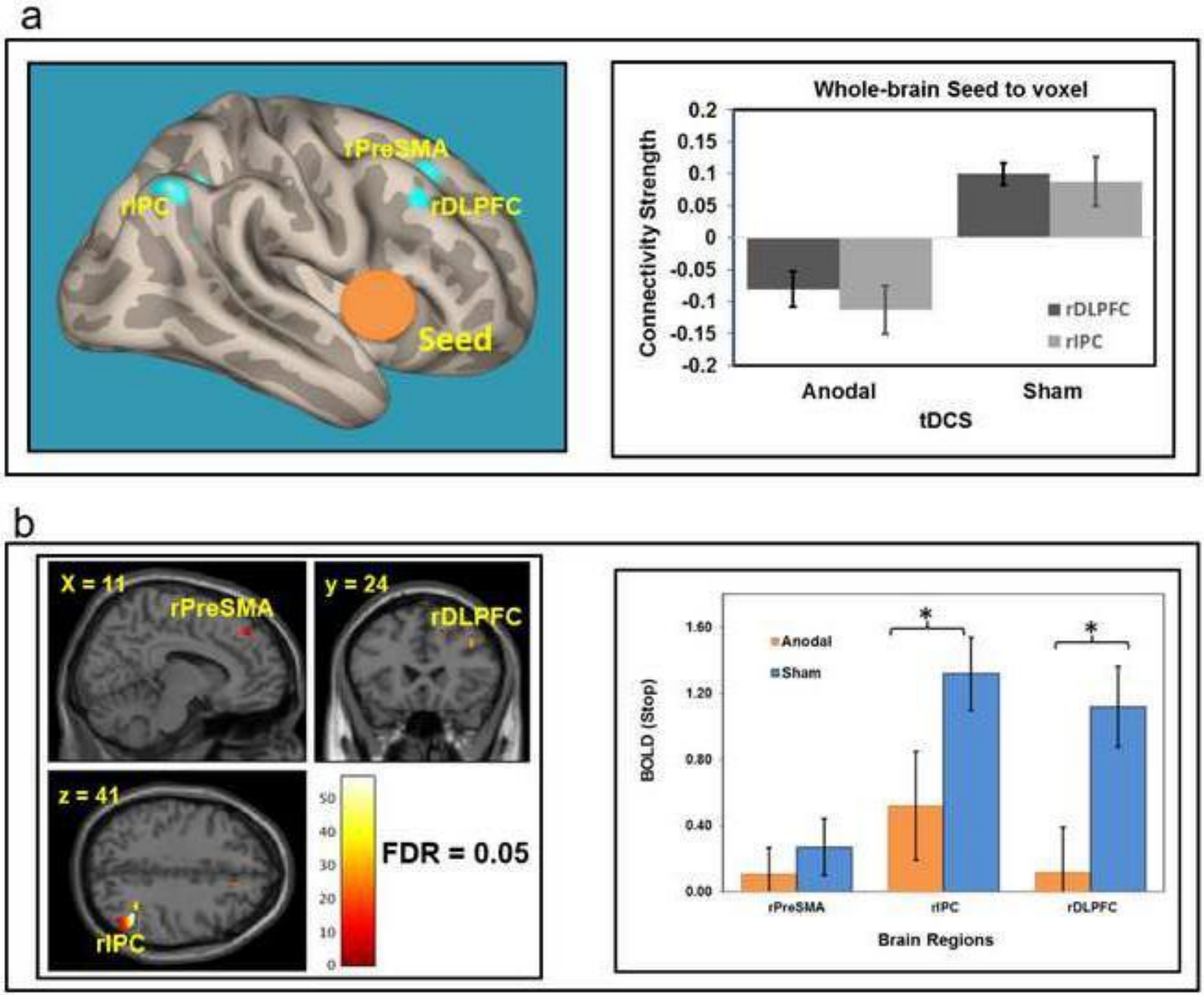

**Table 1.** Behavioral data of the Stop-Signal task

| tDCS | Go RT | | SSRT | |
|---|---|---|---|---|
| | Session 1 | Session 2 | Session 1 | Session 2 |
| **Sham** | 472 ms (± 76) | 493 ms (± 44) | 221 ms (± 32) | 286 ms (± 37) |
| **Anodal** | 446 ms (± 35) | 471 ms (± 49) | 234 ms (± 29) | 274 ms (± 24) |

**Table 2.** Multiple linear regression analyses with SSRT (from the stop-signal task during efMRI) as the dependent variable and the efMRI BOLD activation clusters as the predictor variables.

**a.**

| Predictor Variables | Coefficient | Std Error | T | P | Partial $R^2$ | VIF |
|---|---|---|---|---|---|---|
| Constant | 281.160 | 6.79213 | 41.39 | 0.000 | | 0.0 |
| rPreSMA (Go) | 30.1464 | 19.3302 | 1.56 | 0.147 | 0.17 | 2.1 |
| rIPC (Go) | 48.9783 | 20.5105 | 2.39 | 0.036 | 0.34 | 9.4 |
| rDLPFC (Go) | -60.6819 | 2.5923 | -2.59 | 0.021 | 0.40 | 10.0 |

$R^2$ = 0.45; Adjusted $R^2$ = 0.29; Mean Square Error (MSE) = 422.67; SD = 20.56

**b.**

| Predictor Variables | Coefficient | Std Error | T | P | Partial $R^2$ | VIF |
|---|---|---|---|---|---|---|
| Constant | 263.220 | 17.4886 | 15.05 | 0.000 | | 0.0 |
| rPreSMA (Stop) | -41.8928 | 16.5353 | -2.53 | 0.028 | 0.37 | 1.8 |
| rIPC (Stop) | 32.4451 | 12.8303 | 2.53 | 0.028 | 0.37 | 1.8 |
| rDLPFC (Stop) | -7.61921 | 9.64603 | -0.79 | 0.446 | 0.05 | 1.2 |

$R^2$ = 0.45; Adjusted $R^2$ = 0.30; Mean Square Error (MSE) = 940.43; SD = 30.6

Notes: Table 2a shows the results of the multiple regression analysis with the efMRI BOLD activation clusters during Go responses in the Anodal tDCS group as the predictor variables. Table 2b shows the multiple regression results with the efMRI BOLD activation clusters during Stop responses in the Sham group as the predictor variables. VIF= variance inflating factor; rPreSMA= right pre-supplementary motor area; rIPC= right inferior parietal cortex; rDLPFC= right dorsolateral prefrontal cortex.

***Conflict / Declaration of Interest form**

**Click here to download Conflict / Declaration of Interest form: Conflict of Interest Form (5 signatures).pdf**

**Conflict of Interest Form 2**

**Click here to download Conflict / Declaration of Interest form: Conflict of Interest Form (Volochayev) 03-23-19.pdf**

**Conflict of Interest Form 3**

**Click here to download Conflict / Declaration of Interest form: Conflict of Interest Form (Cohen) 03-23-19.pdf**